Bioorganic & Medicinal Chemistry Letters 22 (2012) 6947–6951

Contents lists available at SciVerse ScienceDirect

Bioorganic & Medicinal Chemistry Letters

journal homepage: www.elsevier.com/locate/bmcl

Design, synthesis and anticancer activity of 1-acyl-3-amino-1,4,5,6-tetrahydropyrrolo[3,4-*c*]pyrazole derivatives

Xiao-Guang Bai [a,†], Dong-Ke Yu [a,†], Ju-Xian Wang [a], Hao Zhang [a], Hong-Wei He [a], Rong-Guang Shao [a], Xue-Mei Li [b,*], Yu-Cheng Wang [a,*]

[a] *Institute of Medicinal Biotechnology, Chinese Academy of Medical Sciences and Peking Union Medical College, Beijing 100050, PR China*
[b] *Center for Drug Evaluation, State Food and Drug Administration Office of Generic Drug Pharmaceutical Science, Beijing 100038, PR China*

ARTICLE INFO

Article history:
Received 15 July 2012
Revised 28 August 2012
Accepted 30 August 2012
Available online 8 September 2012

Keywords:
3-Aminopyrazole
Synthesis
Anticancer activity
CDK5
GSK3β

ABSTRACT

A series of novel 1-acyl-3-amino-1,4,5,6-tetrahydropyrrolo[3,4-*c*]pyrazole derivatives were designed and synthesized. These derivatives were initially evaluated for their in vitro anticancer activity against human colon carcinoma HCT-116 cell line, and compounds **11a**, **b** were chosen for further evaluation their in vitro activity against other five human cancer cell lines. These results indicate that most of the target compounds have considerable in vitro anticancer activity. The most active compound **11a** was found to be 4- to 28-fold more potent than (*R*)-roscovitine against six human cancer cell lines. In addition, compound **11a** was assessed for its activity against 12 kinases, and then evaluated for its interaction mode by docking experiments with cyclin-dependent kinase 5 (CDK5) and glycogen synthase kinase-3β (GSK3β).

3-Aminopyrazole has been recognized as a privileged template in drug design and discovery[1] and numerous compounds containing the 3-aminopyrazole moiety have been developed as potential anticancer agents (Fig. 1), such as the Aurora kinase inhibitors AZD1152,[2] VX-680[3] and PHA-739358,[4] the CDK2 inhibitor PHA-533533.[5]

As a novel scaffold based on the 3-aminopyrazole, 3-amino-1,4,5,6-tetrahydropyrrolo[3,4-*c*]pyrazole bi-cycle scaffold has been developed as potent Aurora-A and CDK2 inhibitors in the past decade.[4,6–9] According to the co-crystal structures of the bi-cycle derivatives in complex with CDKs,[10] we speculated that the N1 position of the bi-cycle scaffold could be exploited to gain accessibility to one of the CDK ATP-binding subsites, which is called the narrow hydrophobic Phe80 pocket. For example, (*R*)-roscovitine (Fig. 2) was also found to pack nicely into the Phe80 subsite of CDK5 by an isopropyl group and inhibited CDK5/p25 with an IC_{50} of 160 nm.[11] Additionally, carbonyl group is always involved in the interaction formed between the Phe80 subsite and CDK inhibitors such as BMS-265246,[12] UCN-01 and its analogues.[13,14] In order to find out more effective derivatives containing 3-aminopyrazole moiety, we have designed and synthesized a series of novel 1-acyl-3-amino-1,4,5,6-tetrahydropyrrolo[3,4-*c*]pyrazole derivatives by introducing a small hydrophobic acyl group at the N1 position of the 3-aminopyrazole moiety (Fig. 2) and evaluated for their anticancer and kinase inhibitory activities. Meanwhile, the Structural–Activity Relationship (SAR) and interaction modes of this kind of compounds were also concluded.

As shown in Figure 2, the novel 1-acyl-3-amino-1,4,5,6-tetrahydropyrrolo[3,4-*c*]pyrazole scaffold was divided into three domains for structural modification and optimization. The substituents at N5-position were first fixed as *N*-butyl carbamyl or benzoyl groups.[4,6–8] The substituents at C3–NH position of the pyrazole ring were mainly from substituted benzoyl groups, similar to the 2,6-dichlorobenzoyl group of AT-7519 (CDK 2 inhibitor).[15] The substituents at N1-position were mainly from small hydrophobic acyl groups.

Synthetic pathway to the novel of 1-acyl-3-amino-1,4,5,6-tetrahydropyrrolo[3,4-*c*] pyrazole derivatives was outlined in Scheme 1. According to well-established literature procedures,[6–8] the imino group of the pyrazole ring of *tert*-butyl 3-amino-4,6-dihydro-1*H*-pyrrolo[3,4-*c*]pyrazole-5-carboxylate **1**[16] was selectively protected by nucleophilic substitution with ethyl chloroformate to yield compound **2**, and then acylation of the primary amine **2** gave key intermediates **3a**–**e**. Removal of ethoxy carbonyl group of the amides **3a**–**e** and subsequently introduction of acyl groups at the N1-position afforded compounds **5a**–**n**. The *N*-Boc group of **5a**–**n**

* Corresponding authors. Tel.: +86 10 68585566x539 (X.-M.L.); tel./fax: +86 10 63165263 (Y.-C.W.).
E-mail addresses: lixm@cde.org.cn (X.-M. Li), wyc9999@gmail.com (Y.-C. Wang).
† These authors contributed equally to this work.

0960-894X/$ - see front matter © 2012 Elsevier Ltd. All rights reserved.
http://dx.doi.org/10.1016/j.bmcl.2012.08.117

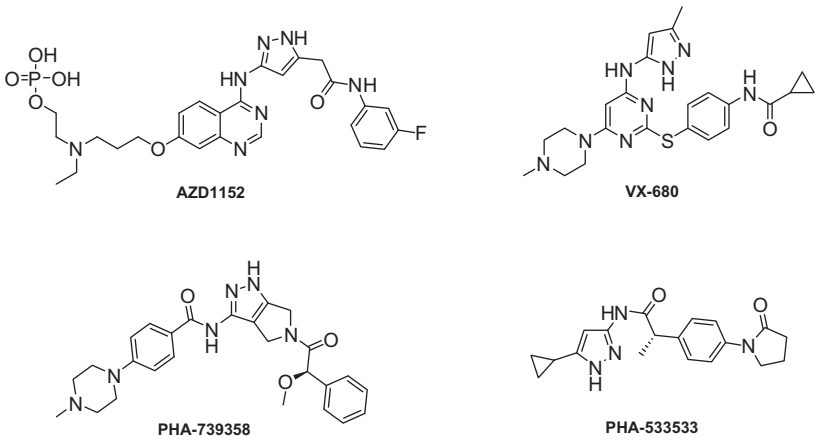

Figure 1. Aurora kinase inhibitors AZD1152, VX-680 and PHA-739358 in clinical trials, CDK2 inhibitor PHA-533533.

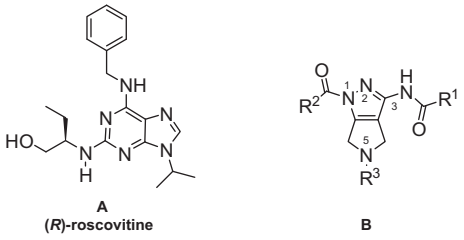

Figure 2. (*R*)-roscovitine (**A**) and chemical structure of 1-acyl-3-amino-1,4,5,6-tetrahydropyrrolo[3,4-*c*]pyrazole scaffold (**B**).

was removed by hydrogen chloride gas or iodotrimethylsilane (TMIS) to give compounds **6a**–**o**, which were finally coupled with butyl isocyanate or the corresponding acyl chlorides to afford the target compounds **10a**–**j**, **11a**–**j** and **12a**–**f**.

However, the acetyl group of **5a** was also partly cleaved simultaneously when reacted with hydrogen chloride gas or TMIS, and this led to the low yields of **11a** (23%, from **3a**) and **12a**–**f** (11–24%, from **3a**). To avoid it, the second synthetic route (Scheme 1) was developed subsequently. The *N*-Boc group of **3a**–**c** was first removed by hydrogen chloride gas to give compounds **7a**–**c**, and introduction of various substituents (R^3) at the N5-positon of **7a**–**c** yielded **8a**–**h** by acylation or sulfonylation. Finally, the other target compounds **12g**–**k** were obtained successfully in improved yields (33–46%, from **3a**) by removal of the ethoxy carbonyl group of **8a**–**h** and subsequently treatment with acetyl chloride.

To evaluate the anticancer activity of these newly synthesized derivatives, the anticancer activity of compounds **10a**–**j**, **11a**–**j** and **12a**–**k** and three precursors **9a**–**c** were initially tested against human colon carcinoma HCT-116 cells by performing SRB assay[17] Compounds **11a** and **11b** were chosen for further evaluation of their anticancer activity against other five human cancer cell lines including HT-29 (colon carcinoma), MCF7 (breast carcinoma), HepG2 (hepatocellular liver carcinoma), A549 (lung carcinoma) and HT-1080 (fibrosarcoma) as well as one normal human liver L02 cell line, respectively. These results were summarized in Tables 1–3, and presented as the concentration of drug inhibition 50% cell growth (IC_{50}). In order to evaluate whether compound **11a** could functionally interfere with the function of the desired protein kinases, it was tested against a panel of 12 human kinases. The result was showed in Table 4 and presented as the inhibition rate (%) at 10 μM concentration.

The target compounds **10a**–**j**, **11a**–**j** and **12a**–**k** and three precursors **9a**–**c** without acyl group at the N1-position were initially evaluated for their in vitro anticancer activity against human colon carcinoma HCT-116 cell line. The 50% inhibition concentrations ($IC_{50's}$) of these compounds along with (*R*)-roscovitine for comparison were presented in Tables 1 and 2.

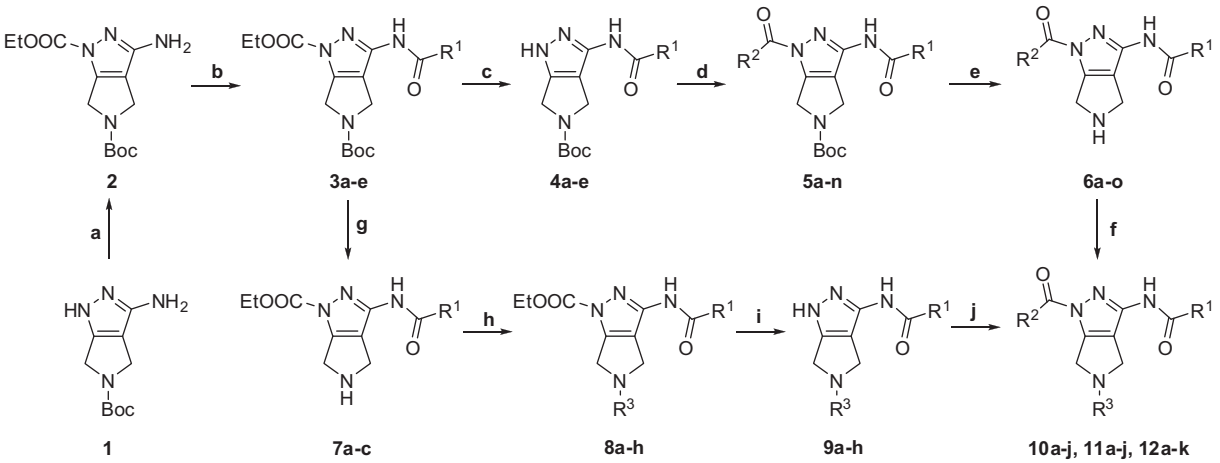

Scheme 1. Reagents and conditions: (a) $ClCO_2Et$, DIEA, THF, 0–5 °C, 12 h; (b) R^1COCl, DIEA, THF, r.t., 12 h; (c) Et_3N, MeOH, r.t., 0.5–3 h; (d) R^2COCl, DIEA, THF, r.t.; (e) HCl (gas), CH_2Cl_2, 0–5 °C, 0.5–2 h or TMSI, $CHCl_3$, N_2, r.t. 20 min, then MeOH, 1 h; (f) *n*-C_4H_9NCO or acyl chlorides, DIEA, CH_2Cl_2, r.t., 5–24 h; (g) HCl (gas), CH_2Cl_2, 0–5 °C, 0.5–2 h; (h) Acyl chlorides or sulfonyl chlorides, DIEA, CH_2Cl_2 or THF, r.t., 24 h; (i) Et_3N, MeOH, r.t., 0.5–3 h; (j) CH_3COCl, DIEA, THF, r.t., 5–12 h.

Table 1
Structure and anticancer activity of compounds **9a–c**, **10a–j** and **11a–j** against HCT-116 cells

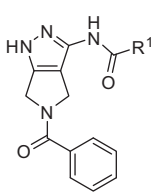

9a-c

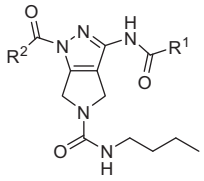

10a-j

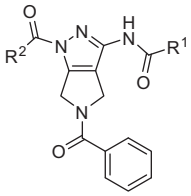

11a-j

Compd.	R^1	R^2	IC_{50}, μM	Compd.	R^1	R^2	IC_{50}, μM
9a	Phenyl	—	6.40	**10j**	Benzyl		43.11
9b	4-F phenyl	—	3.19	**11a**	Phenyl	CH_3—	0.58
9c	4-CH_3O phenyl	—	13.57	**11b**	Phenyl		1.06
10a	Phenyl		3.47	**11c**	Phenyl		2.02
10b	Phenyl		7.47	**11d**	Phenyl		1.24
10c	4-CH_3 phenyl		17.64	**11e**	Phenyl		1.40
10d	4-CH_3 phenyl		23.21	**11f**	Phenyl	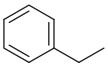	2.61
10e	4-F phenyl		23.25	**11g**	4-F phenyl		2.28
10f	4-F phenyl		30.80	**11h**	4-F phenyl		2.78
10g	4-CH_3O phenyl		65.51	**11i**	4-CH_3O phenyl		5.18
10h	4-CH_3O phenyl		25.28	**11j**	4-CH_3O phenyl		31.30
10i	Benzyl		31.16	(*R*)-roscovitine	—	—	16.38

Table 2
Structure and anticancer activity of compounds **12a–k** against HCT-116 cells

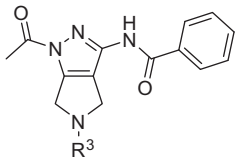

12a-k

Compd	R^3	IC_{50}, μM	Compd	R^3	IC_{50}, μM
12a	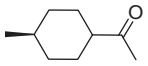	12.16	**12g**	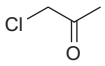	4.10
12b	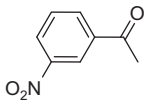	17.29	**12h**		70.29
12c	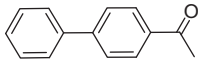	>90	**12i**		35.28
12d	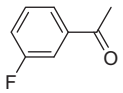	21.94	**12j**	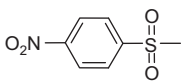	22.29
12e	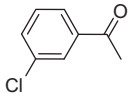	17.41	**12k**	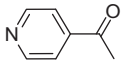	10.04
12f	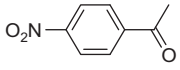	16.19	(*R*)-roscovitine	—	16.38

Table 3
Anticancer activities of compound **11a** against other five human cancer cell lines and one normal human liver L02 cell line

Cell line	IC_{50}, μM		
	11a	**11b**	(*R*)-roscovitine
HT-29	0.92	0.91	11.63
MCF-7	0.99	1.07	12.22
HepG2	0.81	0.86	15.47
A549	1.74	ND[a]	14.14
HT-1080	2.13	ND[a]	9.62
L02	2.22	2.47	20.48

[a] Not detected.

Table 4
Inhibitory activity of **11a** against a panel of 12 human kinases

Kinase	% Inhibition	Kinase	% Inhibition
Aurora-A	33	CDK7/cyclinH/MAT1	5
Aurora-B	32	CDK9/cyclin T1	10
CDK1/cyclinB	30	EGFR	8
CDK2/cyclinA	17	GSK3β	67
CDK2/cyclinE	30	mTOR	3
CDK5/p25	72	PDK1	10

The data listed in Tables 1 and 2 indicated that the tested compounds have generally considerable potency in inhibiting the growth of HCT-116 cell line. Among them, **9a–c**, **10a–b**, **11a–i** and **12a**, **g**, **k** (IC_{50}: 0.58–13.57 μM) were more active than (*R*)-roscovitine (IC_{50}: 16.38 μM). Particularly, the most active compound **11a** (IC_{50}: 0.58 μM) was found to be 28 fold more potent than (*R*)-roscovitine against HCT-116. *N5*-benzoyl derivatives were generally more active than the corresponding N5-*n*-butyl carbamoyl analogues (**11d** vs **10a**, **11e** vs **10b**, **11g** vs **10e**, **11h** vs **10f**, **11i** vs **10g**).

Compound **10a** or **10b** bearing a benzamido group at the C3-position showed higher potency than the corresponding substituted benzamido analogues (**10c**, **e**, **g** or **10d**, **f**, **h**), which was consistent with that of compounds **11d–e** and **11g–j**. It indicated that introduction of an electron-withdrawing or donating group on the *para*-position of the phenyl ring (R^1) such as methyl, methoxyl or fluoro would be detrimental to the activity.

The size of R^2 groups of the acyl moiety at the N1-position was considered to be a factor in determining activity. The relative contribution of R^2 groups to activity was generally as follows: methyl > ethyl > cyclopropyl > phenyl > benzyl. Indeed, compound **11a** with the smallest R^2 group (CH_3) showed the best activity among all of the target compounds. In addition, N1-acyl derivatives **11a–f**, **11g–h** and **11i** showed increased activity than the corresponding N1-des-acyl analogues **9a**, **9b** and **9c**, supporting the importance of the acyl functional group at this position with respect to anticancer activity and the validity of our strategy.

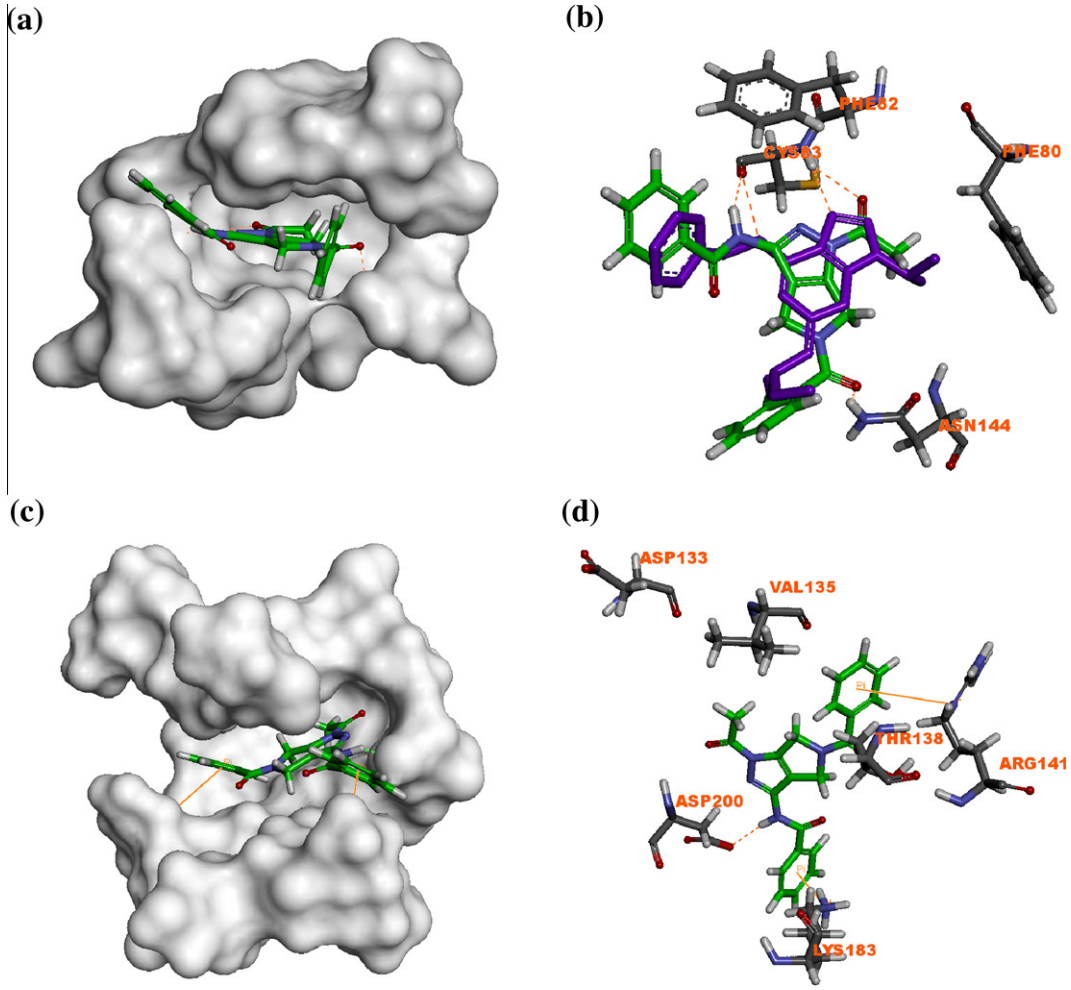

Figure 3. The predicted binding mode for **11a** (stick model) modeled in the ATP-binding pockets of CDK5 (PDB 1UNL) and GSK3β (PDB 1UV5), respectively. (a) Docking model of **11a** to the ATP-binding pocket of CDK5, (b) Overlap of **11a** (atom-type colored) with (*R*)-roscovitine (in purple stick) in CDK5, H-bond (orange dashes). (c) Docking model of **11a** to the ATP-binding pocket of GSK3β. (d) Binding mode of **11a** with GSK3β, H-bond (orange dashes), π–π interaction (orange line).

The above results suggested that acetyl and benzamido groups were the optimal substituents at the N1- and C3-positions in this study, respectively. In order to define more clearly the effect the substituent at the N5-position on the activity, the benzoyl moiety at the N5-position of the most active compound **11a** was also replaced with other acyl and sulfonyl groups (Table 2). When directly compared with **11a**, these derivatives **12a**–**k** showed remarkably decreased activity, although some of them (**12a**, **f**, **g**, **k**) were more active than (*R*)-roscovitine against HCT-116.

Compounds **11a** and **11b** were further evaluated for their in vitro anticancer activity against other five human cancer cell lines including HT-29, MCF7, HepG2, A549 and HT-1080 as well as one normal human liver L02 cell line. The data in Table 3 indicated that **11a** and **11b** have more remarkable anticancer activity against the five human cancer cell lines and human colon carcinoma HCT-116 cell line (Table 1) (IC_{50}: 0.58–2.13 μM) compared with (*R*)-roscovitine (IC_{50}: 9.62–16.38 μM). On the other hand, compound **11a** showed promising anticancer activity on the six human cancer cell lines than normal human liver L02 cell line (IC_{50}: 2.22 μM), which is consistent with (*R*)-roscovitine.

Finally, **11a** was assessed for its activity against a panel of 12 kinases at 10 μM concentration. The data in Table 4 indicated that **11a** has much better activity against CDK5/p25 and GSK3β (72% and 67% of inhibition rates, respectively) than the other ten kinases (3–33% of inhibition rates).

To further understand the binding mode of compound **11a** with CDK5 or GSK3β, molecular docking was performed through CDOCKER module in Discover studio (Fig. 3). Compound **11a** packs nicely into the ATP binding pockets of both CDK5 and GSK3β (Fig. 3a and 3c). The superimposition of the binding modes of **11a** and (*R*)-roscovitine in the ATP binding pocket of CDK5 was shown as Figure 3b. The acetyl of **11a** and the isopropyl of (*R*)-roscovitine form similar hydorphobic interactions with the narrow hydrophobic pocket around residue Phe80. Furthermore the C-3-benzamido and *N*-5-benzoyl moieties of **11a** shows similar orietation as the *N*-6-benzyl and 1-ethyl-2-hydroxyethylamino moieties of (*R*)-roscovitine, respectively, and the 1-acyl-3-aminopyrazole moiety of **11a** also forms two critical H-bonds with residue CYS83. A third H-bond formed between *N*-5-benzoyl moiety of **11a** and residue ASN144. Shown as Figure 3d, there is only one H-bond formed between C-3 amino group and the oxygen of ASP200 residue of GSK3β. Meanwhile, C-3-benzamido and *N*-5-benzoyl moieties of **11a** form two π–π interactions with residues LYS183 and ARG141, respectively. The π–π interaction formed between the phenyl moiety of **11a** *N*-5-benzoyl group and the C=NH of residue ARG141, which is consistent to previous modeling studies that the ARG141 residue (GSK3β) appears to be unique to GSK3β and the interactions with it are benefitial to the selectivity of GSK3β inhibitors.[18,19]

In summary, a series of novel 1-acyl-3-amino-1,4,5,6-tetrahydropyrrolo[3,4-*c*] pyrazole derivatives was designed, synthesized and characterized by ^{1}H NMR, ^{13}C NMR, MS and HRMS. These derivatives and three precursors were evaluated for their in vitro anticancer activity. The results showed that all the tested compounds have generally considerable activity against HCT-116. The activity of compound **11a** (IC_{50}: 0.58–2.13 μM) was found to be 4- to 28-fold more potent than that of (*R*)-roscovitine (IC_{50}: 9.62-16.38 μM) against the six human cancer cell lines. In addition, **11a** has promising inhibitory activity against both CDK5/p25 and GSK3β. Docking results found that **11a** share the similar interaction mode with CDK5 as (*R*)-roscovitine, **11a** also formed hydrogen bond and π–π interactions with GSK3β. Further pharmacological studies of **11a** are currently in progress and will be reported in due course.

Acknowledgments

We are grateful to the financial support from the National S&T Major Special Project on Major New Drug Innovation (2012ZX093101002-001-017) and the National Natural Science Foundation of China (No. 81072577 and 81102376).

Supplementary data

Supplementary data associated with this article can be found, in the online version, at http://dx.doi.org/10.1016/j.bmcl.2012.08.117.

References and notes

1. Anwara, H. F.; Elnagdic, M. H. *Arkivoc* **2009**, *1*, 198.
2. Boss, D.; Witteveen, P.; Van Der Sar, J.; Lolkema, M.; Voest, E.; Stockman, P.; Ataman, O.; Wilson, D.; Das, S.; Schellens, J. *Ann. Oncol.* **2011**, *22*, 431.
3. Tyler, R. K.; Shpiro, N.; Marquez, R.; Eyers, P. A. *Cell Cycle* **2007**, *6*, 2846.
4. Cohen, R. B.; Jones, S. F.; Aggarwal, C.; von Mehren, M.; Cheng, J.; Spigel, D. R.; Greco, F. A.; Mariani, M.; Rocchetti, M.; Ceruti, R. *Clin. Cancer Res.* **2009**, *15*, 6694.
5. Pevarello, P.; Brasca, M. G.; Orsini, P.; Traquandi, G.; Longo, A.; Nesi, M.; Orzi, F.; Piutti, C.; Sansonna, P.; Varasi, M. *J. Med. Chem.* **2005**, *48*, 2944.
6. Fancelli, D.; Berta, D.; Bindi, S.; Cameron, A.; Cappella, P.; Carpinelli, P.; Catana, C.; Forte, B.; Giordano, P.; Giorgini, M. L. *J. Med. Chem.* **2005**, *48*, 3080.
7. Fancelli, D.; Moll, J.; Varasi, M.; Bravo, R.; Artico, R.; Berta, D.; Bindi, S.; Cameron, A.; Candiani, I.; Cappella, P. *J. Med. Chem.* **2006**, *49*, 7247.
8. Pevarello, P.; Fancelli, D.; Vulpetti, A.; Amici, R.; Villa, M.; Pittala, V.; Vianello, P.; Cameron, A.; Ciomei, M.; Mercurio, C.; Bischoff, J. R.; Roletto, F.; Varasi, M.; Brasca, M. G. *Bioorg. Med. Chem. Lett.* **2006**, *1084*, 16.
9. Shi, J.; Xu, G.; Zhu, W.; Ye, H.; Yang, S.; Luo, Y.; Han, J.; Yang, J.; Li, R.; Wei, Y. *Bioorg. Med. Chem. Lett.* **2010**, *20*, 4273.
10. Liao, J. J. *J. Med. Chem.* **2007**, *50*, 409.
11. Jain, P.; Flaherty, P. T.; Yi, S.; Chopra, I.; Bleasdell, G.; Lipay, J.; Ferandin, Y.; Meijer, L.; Madura, J. D. *Bioorg. Med. Chem.* **2011**, *19*, 359.
12. Misra, R. N.; Xiao, H.; Rawlins, D. B.; Shan, W.; Kellar, K. A.; Mulheron, J. G.; Sack, J. S.; Tokarski, J. S.; Kimball, S. D.; Webster, K. R. *Bioorg. Med. Chem. Lett.* **2003**, *13*, 2405.
13. Johnson, L. N.; De Moliner, E.; Brown, N. R.; Song, H.; Barford, D.; Endicott, J. A.; Noble, M. E. M. *Pharmacol. Therapeut.* **2002**, *93*, 113.
14. Sanchez-Martinez, C.; Shih, C.; Zhu, G.; Li, T.; Brooks, H. B.; Patel, B. K. R.; Schultz, R. M.; DeHahn, T. B.; Spencer, C. D.; Watkins, S. A. *Bioorg. Med. Chem. Lett.* **2003**, *13*, 3841.
15. Wyatt, P. G.; Woodhead, A. J.; Berdini, V.; Boulstridge, J. A.; Carr, M. G.; Cross, D. M.; Davis, D. J.; Devine, L. A.; Early, T. R.; Feltell, R. E. *J. Med. Chem.* **2008**, *51*, 4986.
16. Krasavin, M.; Konstantinov, I. O. *Lett. Org. Chem.* **2008**, *5*, 594.
17. Skehan, P.; Storeng, R.; Scudiero, D.; Monks, A.; McMahon, J.; Vistica, D.; Warren, J. T.; Bokesch, H.; Kenney, S.; Boyd, M. R. *J. Natl. Cancer I.* **1990**, *82*, 1107.
18. Tavares, F. X.; Boucheron, J. A.; Dickerson, S. H.; Griffin, R. J.; Preugschat, F.; Thomson, S. A.; Wang, T. Y.; Zhou, H. Q. *J. Med. Chem.* **2004**, *47*, 4716.
19. Kuo, G. H.; Prouty, C.; DeAngelis, A.; Shen, L.; O'Neill, D. J.; Shah, C.; Connolly, P. J.; Murray, W. V.; Conway, B. R.; Cheung, P. *J. Med. Chem.* **2003**, *46*, 4021.